IEEE Access
Multidisciplinary | Rapid Review | Open Access Journal

Received 16 February 2024, accepted 1 March 2024, date of publication 8 March 2024, date of current version 15 March 2024.

Digital Object Identifier 10.1109/ACCESS.2024.3374109

RESEARCH ARTICLE

Adaptive Control Scheme for Space Debris Capture in the Presence of Mass and Inertia Uncertainty

OLGA-ORSALIA CHRISTIDI-LOUMPASEFSKI, BARIŞ CAN YALÇIN, MAXIME HUBERT DELISLE, XIAO LI, MIGUEL A. OLIVARES-MENDEZ, (Member, IEEE), AND CAROL MARTINEZ

Space Robotics (SpaceR) Research Group, Interdisciplinary Centre for Security, Reliability and Trust (SnT), University of Luxembourg, L-1855 Kirchberg, Luxembourg

Corresponding author: Barış Can Yalçın (bariscan.yalcin@uni.lu)

This work was supported by the Interdisciplinary Centre for Security, Reliability and Trust (SnT)-Space Robotics Research Group (SpaceR) under Luxembourg National Research Fund (FNR)—BRIDGES Funding for "High fidELity tEsting eNvironment for Active Space Debris Removal—HELEN" under Grant BRIDGES2021/MS/15836393.

ABSTRACT This paper proposes an adaptive control scheme for capturing uncooperative space debris having uncertain inertial parameters. Debris parameters may be unknown or uncertain due to limited data or changes in orbit due to collisions. To address this challenge, the proposed scheme integrates an inertial parameter identification law with the impedance control strategy of FlexeS (Flexible Capture System). During the pre-capture phase, motion data is utilized to identify the debris' center of mass (CM), leading to the optimal capture point that minimizes impact moments. During contact, the impedance-controlled actuator(s) is(are) activated while the scheme concurrently provides accurate estimates of the debris mass and inertia, enabling the updating of controller gains and thus ensuring sufficient contact time for successful capture. Hence, the proposed adaptive scheme allows FlexeS to handle the debris parameter uncertainties. The simulation study demonstrates the scheme's effectiveness and necessity. The performance of the proposed adaptive scheme is compared with a non-adaptive scheme. The results affirm the superiority of the adaptive scheme in achieving successful soft capture of uncooperative debris in the presence of mass and inertia uncertainties and highlight its potential for future space debris mitigation missions.

INDEX TERMS Orbital robotics, active space debris removal, robotic capturing mechanism, uncooperative debris, gecko adhesive pads, CubeSat, FlexeS.

I. INTRODUCTION

In the vast expanse of the space environment, the number of space debris of various origins have been dramatically increasing [1], [2], [3], [4], [5]. Space debris an escalating threat to Earth's orbital sustainability [4], [6], [7], [8], [9], [10], [11], [12], [13], [14], [15]. Active Debris Removal (ADR) missions have emerged as a pivotal strategy to counteract this imminent hazard [16]. Capturing mechanisms employed can interact differently with the debris; an Energy-Transfer Classification (ET-Class) of them was presented in [17]. For instance, the *Impact Energy Dissipation (ET2)* class implies a capture with a decrease of energy at the first impact. In this class, among the different strategies, the rigid [18], [19] and flexible [20], [21], [22], [23], [24] robotic capturing mechanisms stand out as the most promising ones for their reliability [25]. In our previous work [26], we propose the integration of these two strategies into a unique concept. The proposed hybrid-compliant system is custom-built to fit a CubeSat. It incorporates active (with linear actuators and impedance controller) and passive (revolute joints with torsional springs) compliance to dissipate the impact energy, ensuring sufficient contact time, and successfully capturing a broader range of space debris.

An ADR mission consists of a succession of several crucial phases, being the capturing phase the most crucial one. In our previous work [26], we proposed a concept for the

The associate editor coordinating the review of this manuscript and approving it for publication was Rosario Pecora.

Capturing Phase. It includes three sub-phases: Pre-Capture (Approach Guidance & Control), Soft-Capture, and Hard-Capture; these are in charge of the approach preparation, the impact absorption and stabilization, and the securing of the debris attachment. During the soft capture phase, the servicer satellite's thrusters are turned on to approach the debris and achieve the first contact. This first interaction between FlexeS' tip and the debris can potentially generate substantial interaction forces. These forces may consequently lead to an unsuccessful soft capture, primarily attributed to the unintended separation of the systems. Hence, the first impact between the capturing mechanism and the debris must occur softly.

To address this challenge, our previous work [26] proposed an impedance-controlled hybrid-compliant FlexeS. Impedance Control (IC) stands out as a widely employed control strategy, regulating the relationship between the mechanism's tip position and the impact force [27], [28]. IC gains can be calculated based on the contact time required for soft capture and based on the knowledge of debris mass. As it was shown, to target a vast range of debris masses, FlexeS' compliance, and thus, the IC gains, must be adaptive.

Moreover, debris inertial parameters may be uncertain due to limited data or changes in orbit due to collisions with other debris causing fragmentation. To address this additional challenge and perform the capturing task with high accuracy, adaptive schemes are required. In [29], a strategy for parameter identification and detumbling of a tumbling target by a space manipulator is developed. The contact force is utilized for identifying the target's inertia parameters and detumbling the target, and a unified hybrid impedance control framework is applied to the space robot to track the desired contact force and motion trajectory. In [30], a methodology for online inertia parameters estimation for space debris captured by a tethered system is presented. It includes mass estimation during the post-capture phase, mass estimation during the first half of retrieval, and offsets and moments of inertia estimation during the middle part of retrieval. In [31], an adaptive control algorithm to produce manipulator motion with minimum disturbance to the base after the capture of an unknown tumbling target, and momentum-based inertial parameter identification, are proposed. Hence, although references exist for adaptive approaches in ADR missions, the current literature, to the authors' knowledge, lacks of adaptive schemes specifically designed to ensure the successful soft-capture of space debris employing a robotic capturing strategy, as defined by ET-Class [17].

The novelty of the paper is based on the development of an adaptive control scheme for capturing uncooperative space debris in the presence of debris inertial parameter uncertainty. The proposed scheme integrates the IC control strategy employed by the ADR robotic mechanism presented in [26] with an identification law that estimates the required debris inertial parameters. From this point of view, the proposed controller is tailor for FlexeS oriented ADR robotic mechanism. During the pre-capture phase, the debris' center of mass is estimated using motion data, allowing the calculation of the optimal capture point that minimizes impact moments. During the contact, the impedance-controlled actuators of the robotic mechanism are activated while accurate debris mass is concurrently estimated. Controller gains are updated during the capture phase, ensuring sufficient contact time for the successful completion of soft capture using gecko-adhesive pads. Gecko-adhesive pad's adhesive property is sensitive to contact time, so that the estimation of mass and adapting the stiffness and damping coefficients accordingly has crucial importance. Thus, the proposed adaptive scheme allows FlexeS to handle debris with uncertainties in their inertial parameters.

The structure of the paper is given as follows; The capture phase, hybrid-compliant robotic capturing system, soft capture process and system modeling are mentioned in Section-II. Impedance control law, adaptive controller gains and parameter identification law are given in Section-III. Identification and adaptive control results are shown in Section IV, and finally the conclusion is stated in Section-V.

II. SPACE DEBRIS CAPTURE

A. THE CAPTURING PHASE

An ADR mission consists of several phases, the capturing phase being the most crucial. Mission failure and debris generation can occur more easily during that phase, and the consequences can be dramatic.

The Capturing Phase includes three sub-phases: Pre-Capture, Soft-Capture, and Hard-Capture [26]; these are in charge of the approach preparation, the impact absorption and stabilization, and the securing of the debris attachment. This paper focuses on the Soft Capture sub-phase. In this sub-phase, the servicer satellite's thrusters are turned on to approach the debris and achieve the first contact. The first impact between the capturing mechanism and the debris must occur softly to ensure that the debris is not pushed away and give enough contact time for the capture.

B. HYBRID-COMPLIANT ROBOTIC CAPTURING SYSTEM

The high demand for reliability while capturing uncooperative debris requires compliant robotic systems. This paper employs a hybrid-compliant robotic system for Soft Capture developed at a conceptual level and presented in [26]. With passive and active compliance while fitting into a CubeSat architecture, as displayed in Figure 1, this robotic capturing system considers the capturing of uncooperative small box-shaped debris in Low Earth Orbit (LEO). As shown in Figure 1, the robotic system combines passive and active compliant units, denoted as Passive Compliance Unit (PCU) and Active Compliance Unit (ACU), respectively, to reduce shocks, hard contacts, and residual vibrations and actively control the contact time to avoid motion-reaction effects.

- The PCU has two main functions: to ensure a softer impact with the debris and to adhere to the debris

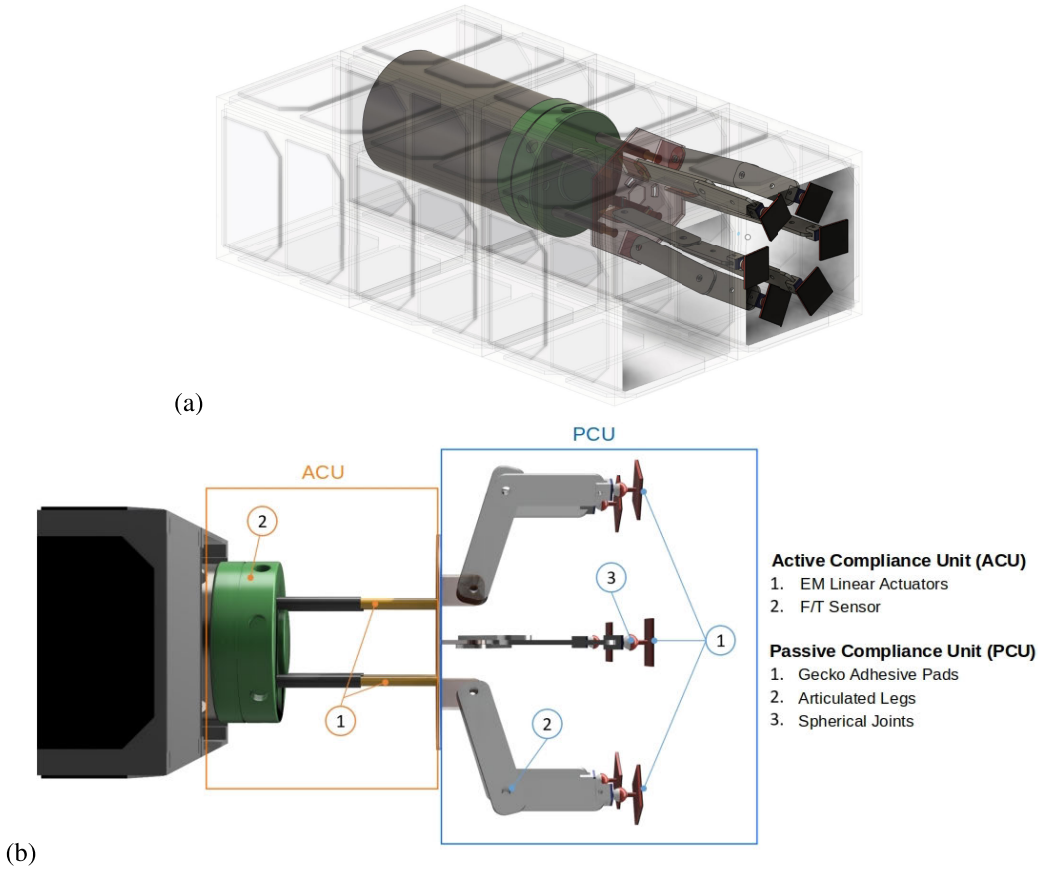

FIGURE 1. (a) FlexeS folded inside a 3U CubeSat. (b) Closeup of the system, including the ACU and the PCU.

surface, both preventing it from moving away. This unit consists of flexible legs, spherical joints, and adhesive pads.

- The ACU is directly linked to the PCU with a plate. This unit consists of four linear actuators, all linked with their base to a Force/Torque (F/T) sensor. Active compliance is ensured thanks to the active control of the linear actuators along the capture axis. Details about the controller are presented in III-A. By actively changing the stiffness of the ACU, it is possible to ensure a sufficient contact time to actuate the other parts of the ADR capturing process. This allows the system to target a wider range of debris without fundamentally changing its conceptual design.

C. SOFT CAPTURE PROCESS

The robotic system approaches the debris, translating in the target's axis. At this moment of the mission, the system is fully deployed and ready to impact the debris as softly as possible. The PCU is the part that arrives in contact with the flat surface of the debris first, with its gecko adhesive pads parallel to the debris surface.

As the contact is made, the flexible legs articulate naturally, providing the first damping of the impact's vibrations and not being close to an elastic collision between the two entities (where both momentum and kinetic energy are conserved). The fixed stiffness of the PCU lets the legs articulate while keeping in contact with the debris surface. The gecko adhesive pads are not yet activated at the exact moment of the impact. At this time of the process, the PCU is not the only one acting; the ACU is also activated at the impact.

As soon as there is contact between the Soft Capture Unit (SCU) and the debris, a force is exerted in the axis of the capture on the ADR system's tip. That force is fed into the controller of the ACU. As a result, the electromechanical linear actuators are put into action accordingly, reducing their length, and thus providing another set of virtual springs and dampers based on the contact's force.

The amount of time in which the debris is in contact with the tip of the capturing system, t_c, of the Soft Capture, can then be controlled. The action of passive and active compliance is done within that time frame of t_c seconds, also giving the required theoretical time for the Adhesive Activation to occur, which is essential to the mission's success. As the bond is created, the Hard Capture Unit (HCU) is activated to reliably secure the debris to the servicer satellite, ready for deorbiting. A too-short contact time will not allow the gecko adhesive pads to activate themselves, and the hard capture would not happen, leading to a mission failure.

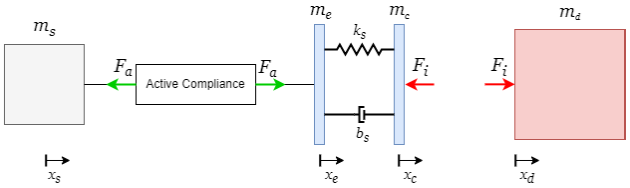

FIGURE 2. Model of the hybrid-compliance.

D. SYSTEM MODELING

The robotic capturing system, consisting of a main body (CubeSat) and the hybrid-compliant FlexeS for soft capture, is modelled as a three-body equivalent system with masses m_s,m_e, and m_c, as represented in Figure 2. m_s is the mass of the satellite, its position is denoted by x_s. As the moving part of the ACU's actuators, the plate that separates ACU and PCU, and the PCU's upper legs are lumped into a second rigid body with mass m_e; while the lower legs and the gecko adhesive pads are lumped to a third rigid body having mass m_c. The CM positions of m_s and m_e are denoted by x_s and x_e, and the position of the mechanism's tip is denoted by x_c. The debris is modelled as a rigid body of mass m_d, and the position of the point on the debris that comes into contact with the mechanism's tip is denoted by x_d.

Masses m_e and m_c are connected through passive compliance, with stiffness k_s of physical length l_s and damping b_s. Masses m_s and m_e are connected through impedance-controlled linear actuators that apply the commanded force F_a on the capture unit, allowing a translation degree of freedom to be controlled. The impact force between the mechanism's tip and the debris is denoted by F_i. All forces are shown in Figure 2. The system equations of Figure 2 are given in Eq. 1, Eq. 2, Eq. 3 and Eq. 4.

$$m_s\ddot{x}_s = -F_a \tag{1}$$
$$m_e\ddot{x}_e = F_a + k_s(x_c - x_e - l_s) + b_s(v_c - v_e) \tag{2}$$
$$m_c\ddot{x}_c = -F_i - k_s(x_c - x_e - l_s) - b_s(v_c - v_e) \tag{3}$$
$$m_d\ddot{x}_d = F_i \tag{4}$$

The state-space representation of the system given in Eq. 5.

$$\frac{\mathbf{dx}}{\mathbf{dt}} = \mathbf{Ax} + \mathbf{B_1u} + \mathbf{B_2w} \tag{5}$$

$\mathbf{A}\in\mathbb{R}^{n\times n}$ is the state matrix in Eq. 6, $\mathbf{B_1}\in\mathbb{R}^{n\times r}$ is the control input matrix in Eq. 7 and $\mathbf{B_2}\in\mathbb{R}^{n\times p}$ is the exogenous input matrix in Eq. 8. F_i is modelled as the disturbance input, F_a is modelled as the controller output.

$$\mathbf{A} = \begin{bmatrix} 0 & 0 & 1 & 0 \\ 0 & 0 & 0 & 1 \\ -k_s/m_e & k_s/m_e & -b_s/m_e & b_s/m_e \\ k_s/m_c & -k_s/m_c & b_s/m_c & -b_s/m_c \end{bmatrix} \tag{6}$$

$$\mathbf{B_1} = \begin{bmatrix} 0 \\ 0 \\ -1/m_e \\ 0 \end{bmatrix} \tag{7}$$

$$\mathbf{B_2} = \begin{bmatrix} 0 \\ 0 \\ 0 \\ 1/m_c \end{bmatrix} \tag{8}$$

where

$$\mathbf{x} = \begin{bmatrix} x_e \\ x_c \\ \dot{x}_e \\ \dot{x}_c \end{bmatrix} \tag{9}$$
$$u = F_a \tag{10}$$
$$w = F_i \tag{11}$$

III. ADAPTIVE CONTROL SCHEME

To effectively clear space debris, a servicer CubeSat must execute a sequence of crucial tasks: final approach, FlexeS deployment, and the capture phase of the ADR mission. Having a hybrid-compliant robotic system demands the development of the appropriate controller, particularly in the presence of uncertainties. In this section, the aim is to precisely control the interaction between the FlexeS' tip and contact force during the soft-capture phase. This is achieved by implementing an impedance controller, which proves valuable when dealing with uncertain or unknown debris masses. To meet this challenge, the control law that relies on model information, here the debris mass, is utilized in conjunction with an identification law, ultimately resulting in an indirect adaptive controller [32].

A. IMPEDANCE CONTROL LAW

For successful capture, the required contact time between the FlexeS' tip and the debris must be ensured; thus, its adjustment is required. This adjustment is achieved by altering the robotic system's impedance. Therefore, an impedance controller with tunable gains is employed.

Subsequently, the controller needs to be informed which is the desired relation between the robotic system's variables during impact i.e. the desired system's behaviour. The equation selected to describe this behaviour is called *impedance filter* and is shown in Eq. (12), [33], [34]. It consists of three terms: one for the desired inertia m_f to be seen at the tip, one for the desired damping b_f, i.e. the desired relationship between contact force and tip's velocity, and one for the desired stiffness k_f, i.e. the desired relationship between contact force and tip's displacement [27].

$$m_f(\ddot{x}_c - \ddot{x}_s) + b_f(v_c - v_s) + k_f(x_c - x_s - l_m) = -F_i \tag{12}$$

The desired contact time of the FlexeS with the debris and, thus, the success of capturing directly, can be realized by tuning the mass, spring, and damper impedance parameters m_f, b_f, and k_f, respectively. Parameter l_m in Eq. (12) is the initial distance between m_c and m_s.

Combining the system equations of motion and the impedance filter, then solving for the applied actuator force by the impedance controller F_a required to achieve the desired impedance behaviour, and selecting the impedance parameter

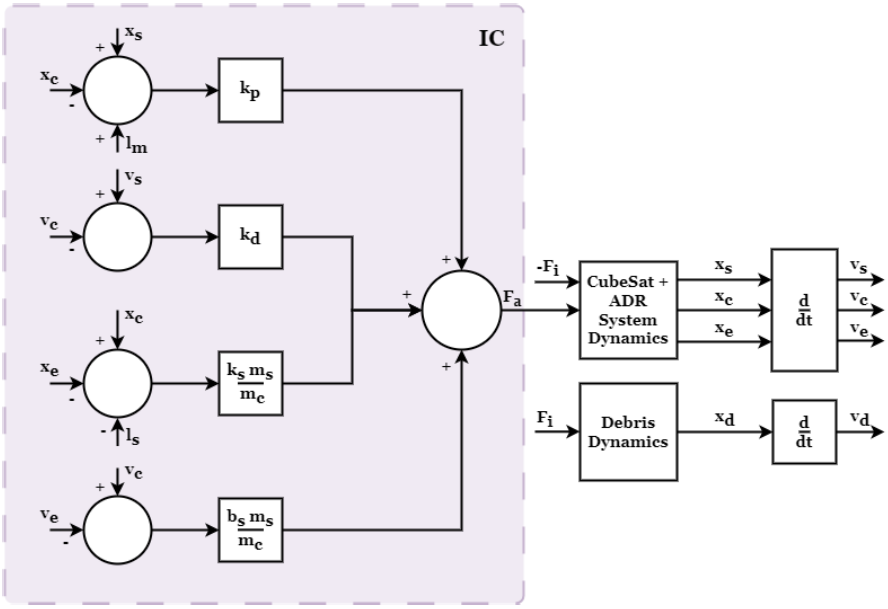

FIGURE 3. Block diagram of the impedance control strategy for the soft capture of space debris.

m_f equal to m_c so that the actuator force F_a does not depend on the impact force F_i [34], yields

$$F_a = k_p(x_s - x_c + l_m) + k_d(v_s - v_c) + \frac{m_s}{m_c}k_s(x_c - x_e - l_s) + \frac{m_s}{m_c}b_s(v_c - v_e) \quad (13)$$

where the controller's gains k_d,k_p are given by

$$k_p = \frac{m_s}{m_c}k_f, k_d = \frac{m_s}{m_c}b_f \quad (14)$$

The impedance control loop is shown as a block diagram in Figure 3.

B. ADAPTIVE CONTROLLER GAINS

To calculate the gains based on Eq. (14), the impedance parameters k_f, and b_f of Eq. (12) must be selected. The desired spring and damper parameters of the impedance filter k_f and b_f can be calculated as

$$k_f = \frac{m_f}{\mu_{ef}}k_m, b_f = \frac{m_f}{\mu_{ef}}b_m \quad (15)$$

where the desired mass parameter m_f is equal to m_c, as Section III-A mentions, and μ_{ef} is given by

$$\mu_{ef} = \frac{m_c m_s}{m_c + m_s} \quad (16)$$

The desired stiffness and damping coefficients k_m and b_m of the hybrid system's equivalent compliance to ensure a specific minimum contact time with a debris of specific mass are selected based on the authors' previous work [26]. Since the debris mass may be uncertain for several reasons, the parameter identification law in Section III-C identifies the debris mass.

Using the impedance parameters m_f, b_f, and k_f derived based on the identified debris mass, the IC gains k_p and k_d can be calculated based on Eq. (14).

C. PARAMETER IDENTIFICATION LAW

The proposed identification law is developed for implementation during the pre-capture and soft-capture sub-phases. This method will focus on the observation of debris motion and contact force. It employs a kinematic equation for velocity and the impulse-momentum equation and collects measurements before and during contact from a perception system and a force sensor. Both are assumed to be part of the robotic system. Using a least-squares algorithm, the knowledge of the required debris inertial parameters is obtained to become available to the control strategy for safe and reliable capture of the debris.

1) IDENTIFICATION OF CENTER OF MASS

In this stage, FlexeS is already deployed. While it is approaching the debris, it is assumed that a perception system mounted on the robotic system tracks the 3D position of a feature point on the surface of the debris.

An observation frame p is attached to a feature point P on the debris, shown in Figure 4. For short experiment times and neglecting microgravity and orbital mechanics effects, a local frame that rotates at the orbital speed can be considered an inertial frame i.

In this identification step, the required measurements to be employed by the identification law are the linear velocity $\mathbf{v}_p$, the attitude $\boldsymbol{\varepsilon}_p$, η_p, and the angular velocity ω_p of frame p, i.e., the frame on the debris that the Servicer's perception system tracks, see Figure 4.

The linear velocity $\mathbf{v}_p$ can be represented by the following kinematic equation

$$\mathbf{v}_p = \mathbf{v}_{cm} + \omega_p \times \mathbf{R}_p{}^p\mathbf{r}_{p/cm} \quad (17)$$

where $\mathbf{v}_{cm}$ is the debris CM velocity, which remains constant when the debris is free-floating. Normally

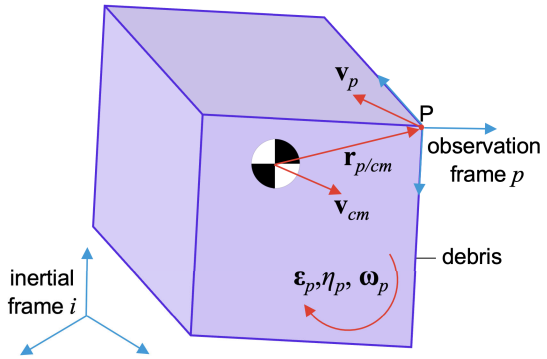

FIGURE 4. Debris' feature point and observation frame schematically.

distributed Gaussian random signal having 0.1 magnitude variance is added to $\mathbf{v}_{cm}$. $\mathbf{r}_{p/cm}$ is the vector from debris CM to frame p, $\mathbf{R}_p(\boldsymbol{\varepsilon}_p, \eta_p)$ is the rotation matrix, which represents the orientation of frame p with respect to the inertial frame, expressed as a function of the Euler parameters $\boldsymbol{\varepsilon}_p, \eta_p$, and $(\cdot)\times$ stands for the cross product skew-symmetric matrix of $(\cdot)$. Vector $\mathbf{r}_{p/cm}$ is considered as an unknown parameter to be estimated by the identification law; once estimated, it renders the debris CM known.

While the debris is rotating in free-floating mode during the pre-capture phase, N measurements are used at time instants $t_1, t_2, \ldots, t_N$ of frame's p position $\mathbf{r}_p$ and attitude $\boldsymbol{\varepsilon}_p, \eta_p$. The position can differentiated to obtain linear velocity $\mathbf{v}_p$. The quaternions $\boldsymbol{\varepsilon}_p, \eta_p$ can be differentiated, and the angular velocity can be calculated by solving the following equation for ω_p [35],

$$\begin{bmatrix} \dot{\boldsymbol{\varepsilon}}_p \\ \dot{\eta}_p \end{bmatrix} = \frac{1}{2}\mathbf{R}_p^T \begin{bmatrix} \boldsymbol{\varepsilon}_p{}^{\times} + \eta_p \mathbf{I}_3 \\ -\boldsymbol{\varepsilon}_p^T \end{bmatrix} \omega_p \tag{18}$$

where $\mathbf{I}_3$ is the 3×3 identity matrix. Hence, the following system of equations arises, written in a matrix form as

$$\bar{\mathbf{A}}\bar{\mathbf{x}} = \bar{\mathbf{b}} \tag{19}$$

where

$$\bar{\mathbf{A}} = \begin{bmatrix} \mathbf{I}_3 & \omega_p(t_1)^{\times}\mathbf{R}_p(t_1) \\ \mathbf{I}_3 & \omega_p(t_2)^{\times}\mathbf{R}_p(t_2) \\ \cdots & \cdots \\ \mathbf{I}_3 & \omega_p(t_N)^{\times}\mathbf{R}_p(t_N) \end{bmatrix} \tag{20}$$

$$\bar{\mathbf{x}} = \begin{bmatrix} \mathbf{v}_{cm} \\ {}^{p}\mathbf{r}_{p/cm} \end{bmatrix} \tag{21}$$

$$\bar{\mathbf{b}} = \begin{bmatrix} \mathbf{v}_p(t_1) \\ \mathbf{v}_p(t_2) \\ \cdots \\ \mathbf{v}_p(t_N) \end{bmatrix} \tag{22}$$

To solve for $\bar{\mathbf{x}}$, a nonzero angular velocity i.e. rotating debris, and measurements of at least two-time instants, are required. In the presence of noise, more measurements are required and as informative as possible. The system in Eq. (19) is overdetermined and can be solved using a least-squares algorithm. Thus, the object's CM and CM velocity can be estimated at any time while the system is free-floating.

Based on the identified debris CM, the optimal point for contact can be determined by aligning the contact force to traverse through the debris CM, thereby minimizing the impact moment, ideally reducing it to zero.

2) IDENTIFICATION OF MASS

This identification step takes place during the soft-capture phase. It is assumed that a perception system is mounted on the robotic capturing system and tracks a debris's feature point's linear velocity. The debris CM velocity can be identified at each time step by solving Eq. (17) and using the identified parameter vector $\mathbf{r}_{p/cm}$ in Section III-C1. The soft-capture phase starts with the pad applying a small impulse to the debris. A force sensor is mounted either on the robotic system's base (CubeSat) or the robotic system's end-effector (FlexeS' pad) and measures the impact force. During the contact, the impulse is calculated for each time step; the impulse that acts on the debris is the opposite one. The estimation of the mass is based on the impulse-momentum equation

$$m_d \mathbf{v}_{cm}(t_1) + \int_{t_1}^{t} \mathbf{F}_i \, dt = m_d \mathbf{v}_{cm}(t) \tag{23}$$

where m_d is the debris mass, and $\mathbf{F}_i$ is the impact force applied on the debris. The debris CM velocity is constant before the application of the impulse by the FlexeS' pad and is represented in Eq. (23) as $\mathbf{v}_{cm}(t_1)$. The debris CM velocity during the application of the impulse by the pad is represented as $\mathbf{v}_{cm}(t)$ and can be calculated by solving Eq. (17) and using the identified parameter vector $\mathbf{r}_{p/cm}$.

Eq. (23) can be written for the axis of contact, e.g. the y-axis, and solved for m_d,

$$m_d = \frac{\int_{t_1}^{t} F_{i,y} \, dt}{v_{cm,y}(t) - v_{cm,y}(t_1)} \tag{24}$$

Based on the identified debris mass, the controller's gains are updated to ensure sufficient contact time for successful capture. The adaptive control strategy is shown as a block diagram in Figure 5.

IV. SIMULATION RESULTS

A simulation study was conducted to illustrate the proposed adaptive control strategy employed by FlexeS during the soft-capture phase. This study aims to validate the identification law employed and to demonstrate the necessity of its concurrent use with the IC to ensure the required minimum contact time with the debris.

The simulations were run in MATLAB/Simscape. Figure 6 shows the Simscape model consisting of FlexeS mounted on the Servicer CubeSat and the space debris. The FlexeS incorporates a linear actuator. The debris is modelled as a box shape, as predominant shape in LEO [26].To model the contact, the Spatial Contact Force block is used. The simulation is conducted with a 1 ms sampling time and a total duration of 15 seconds.

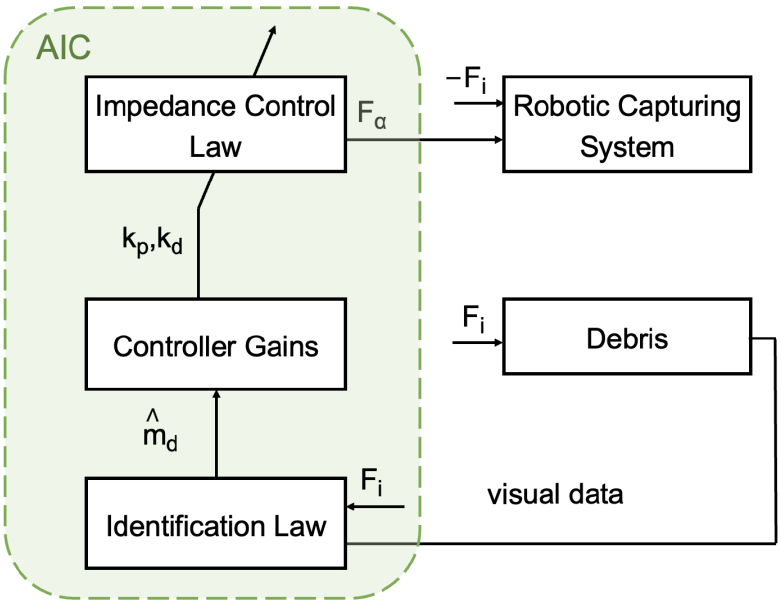

FIGURE 5. Block diagram of the adaptive control strategy.

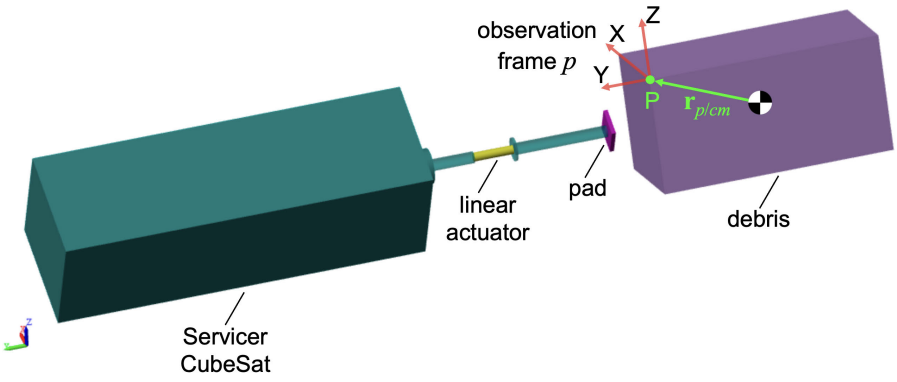

FIGURE 6. Simscape model of FlexeS' simplified visualization and debris.

Equivalent robotic systems' point masses m_s, m_c, and m_e are 12.0012 kg, 0.024 kg, and 0.016 kg, respectively. These values come from the CAD model of the presented hybrid-compliant system. To showcase the necessity of the debris mass identification and the implementation of an adaptive control scheme, a use case is considered with a debris mass of 4 kg.

The FlexeS is already deployed. The pre-capture phase starts with the robotic system approaching the debris with a small non-zero relative velocity equal to 10 mm/s. The debris is tumbling with angular velocity $\omega_p = [0\ 30\ 0]^T$ deg/s, i.e. 30 deg/s about the y-axis shown in Figure 6. The robotic system also rotates about the y-axis; here, at 2 deg/s. Hence, the motion of the two systems is considered synchronized so that the pad's surface is parallel with one of the faces of the box-shaped debris; here, the front face of the debris that lies along the x-z plane, as shown in Figure 6.

While the robotic system is approaching the debris, it is assumed that a perception system mounted on the robotic system provides the pose of an observation frame p attached to the debris. Frame p is chosen to be at one of the debris' corners, as shown in Figure 6, to enhance the identification of its CM. This selection is crucial because, as an observation frame moves farther from the CM, its linear velocity due to rotation increases and subsequently, a higher signal-to-noise ratio is achieved. Based on the perceived motion data while the debris is free-floating in the pre-capture phase, the constant vector ${}^p\mathbf{r}_{p/cm}$ and thus, the location of the debris CM, is identified by solving the system of equations (19) using the least-squares algorithm. To pinpoint the optimal contact point given the parallel faces along the x-z plane of the debris and the pad, only the identified -x and -z components of ${}^p\mathbf{r}_{p/cm}$ are required.

The soft-capture phase starts with the FlexeS' pad interacting with the debris, applying a small impulse to it. Once the systems come into contact, the FlexeS' linear actuator is activated and applies a commanded force F_a driven by the proposed adaptive IC and given by Eq. (13). During

contact, the perception system provides the debris motion data, and a force sensor mounted on the FlexeS provides the impact force measurements. The impulse that acts on the debris is calculated, and the debris mass is identified using Eq. (24) at each time step and employing the recursive least-squares algorithm. Based on the identified debris mass, the controller's gains are updated to ensure sufficient contact time for successful capture, as depicted in Figure 5.

A. IDENTIFICATION RESULTS

To obtain more realistic identification results, sensor noise is introduced into the contact force and debris orientation, linear, and angular velocity signals. The noise is modelled as an additive zero mean white Gaussian noise. Considering that in Gaussian distribution, 99.7% of measurements fall within the first three standard deviations (3σ) of the mean, σ was carefully selected to achieve a meaningful signal-to-noise ratio for identification purposes. Specifically, the 3σ was selected to correspond to 10% of the signal's peak value; thus, a meaningful percentage of noise was used to ensure informative data. Before inputting the noisy measurements into the identification law, measurements undergo filtering via a low-pass Butterworth filter.

In this simulation study, 20 runs with random seed numbers were conducted. Table 1 compares the true inertial parameters (Second column) with the sample mean of the parameters estimated by the identification law (Third column). The corresponding sample Standard Deviation (STD) of the estimated parameters is also presented in the table (Fourth column). The fifth and sixth columns display the sample mean and standard deviation of the estimated parameters' relative error, respectively. The identification results for the debris mass are derived for each time step by the recursive least-squares. The mass identification results in this table correspond to the time instant t=3 s. The results indicate that the identification law produces accurate estimates, with relative errors (sample means) below 5%, in the case of recursive mass identification only after a few seconds of contact, well within acceptable error margins, for all required debris inertia parameters.

TABLE 1. Identification Results.

Parameter	True Value	Sample Mean	Sample Std	Rel. Error Mean	Rel. Error Std
${}^{p}r_{p/cm,x}$	0.05	0.0479	0.0003	4.16	0.52
${}^{p}r_{p/cm,z}$	0.05	0.0481	0.0002	3.76	0.46
m_d	4	4.024	0.085	1.56	1.53

Figure 7 illustrates the estimated value of debris mass and the corresponding relative error, derived using the debris motion data and contact force during the soft-capture phase. From Figure 7, it can be seen that when the soft-capture sub-phase starts, at 2.7 seconds, the algorithm requires a period to collect the necessary amount of sensor data and estimate accurately the system parameters. Nevertheless, within 2 s, the identification error is less than 5%. For 20 runs with random seed numbers, the sample mean time to obtain

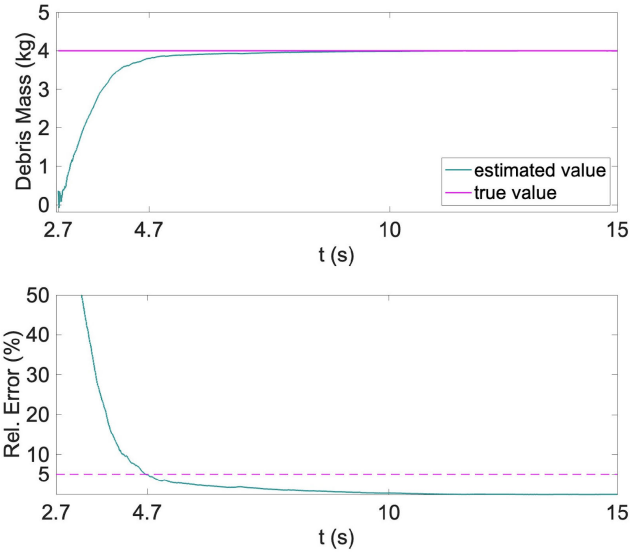

FIGURE 7. Identification Results. (a) Estimated mass, (b) Relative Error (%).

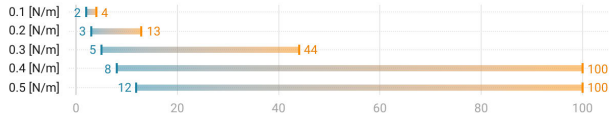

FIGURE 8. Range of debris masses for different stiffness coefficients.

relative errors less than 5% is 1.56 s, and the sample Std is 0.68 s. This fast convergence demonstrates that the method can be used during the operation as long as some minimal motion exists, even a quite slow one.

B. ADAPTIVE CONTROL RESULTS

To demonstrate the improvement of the system response due to the integration of the parameter identification process in the control scheme, the same impedance controller is used, without, though, gains tuning through identification, constantly using the initial and inaccurate debris mass value.

Consider the use case where the initial guess of debris mass value is 12 kg. Assuming that the minimum contact time required for complete capture is 10 s in Figure 8, to target a range of debris masses 12-100 kg, the gains should be k_p = 0.5 N/m, and k_d = 0.42 Ns/m for critical damping.

However, the actual debris mass is 4 kg. The non-adaptive control, which lacks updated knowledge through identification, retains the inappropriate gain values k_p = 0.5 N/m and k_d = 0.42 Ns/m throughout the entire contact phase. In contrast, upon implementing the adaptive control scheme, an accurate estimation of the debris mass is promptly achieved within the initial 2 seconds of contact, as demonstrated in Figure 7. Based on the updated knowledge of debris mass to be 4 kg and using Figure 8, the gain k_p is adjusted to 0.2 N/m, and k_d to 0.17 Ns/m for critical damping, after the first 2 seconds of the contact.

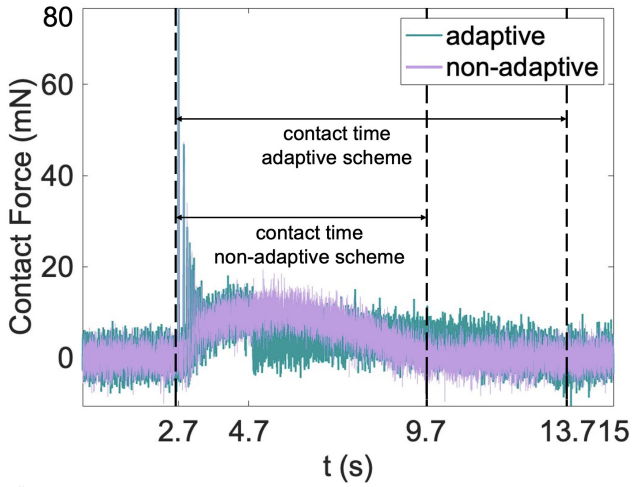

FIGURE 9. Comparison of contact forces of the adaptive and non-adaptive system.

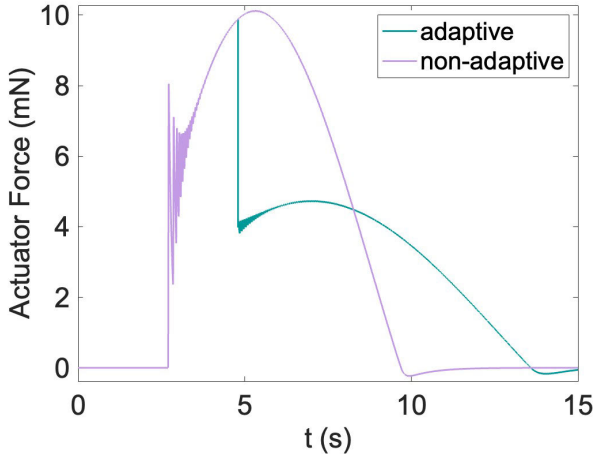

FIGURE 10. Comparison of adaptive and non-adaptive impedanced-controlled actuator forces.

The non-adaptive and adaptive cases were compared. For both non-adaptive and adaptive cases, the responses were measured, and the corresponding contact times were calculated and compared. Figure 9 shows the impact forces generated at the FlexeS' tip with a non-adaptive (light-purple line) and the proposed adaptive control strategy (turquoise line). Figure 10 shows the commanded force by impedance-controlled actuator by a non-adaptive and by the proposed adaptive controller to be less than 80 mN in both cases.

By examining Figure 9 and utilizing the corresponding noiseless contact force signals, we can deduce that in the non-adaptive scenario, the contact initiates at 2.7 seconds and terminates at 9.7 seconds. In contrast, in the adaptive case, the contact lasts until 13.7 seconds. This comparison reveals a substantial increase in contact time, from 7 seconds to 11 seconds, when employing the parameter identification law. Consequently, the adaptive control strategy effectively extends the contact duration between the FlexeS' tip and the debris, ensuring it meets the minimum requirement of 10 seconds. A contact time of 7 seconds would lead to a failure in the mission, as it wouldn't allow for successful capture. However, with an extended contact time of 11 seconds, the robotic mechanism gains ample time to complete the debris capture successfully. This validates the necessity of an adaptive control scheme during the critical capturing phase of an ADR mission.

V. CONCLUSION

This study introduced an adaptive control scheme designed for a robotic capturing mechanism, aimed at ensuring sufficient contact time for the successful capture of space debris characterized by uncertain inertial parameters. The proposed scheme integrates an inertial parameter identification law and an impedance control law, strategically applied during different phases of the capture process. In the pre-capture phase, aligning the contact force to traverse through the debris center of mass (CM) optimally determines the contact point, minimizing the impact moment. Ideally, this reduces to zero with an accurate CM estimate. In the simulation study conducted using MATLAB/Simscape, the CM identification law effectively utilized debris motion data from a perception system mounted on the robotic system, achieving accurate identification of the unknown debris CM with relative errors below 5%. In the soft-capture phase, the adaptive control strategy activates the impedance-controlled actuator(s) while concurrently providing estimates of debris mass using the recursive least-squares algorithm. The controller gains are dynamically updated based on the mass estimate, ensuring sufficient contact time with the debris. The simulation results demonstrated the identification law's ability to accurately estimate debris mass, with relative errors below 5% within a few seconds of contact (sample mean time: 1.56 s, Std: 0.68 s). This fast convergence enables FlexeS to effectively handle debris parameter uncertainties. Comparative analysis including adaptive and non-adaptive strategies highlighted the effectiveness and necessity of the proposed adaptive approach. The adaptive control strategy significantly extended the contact duration between FlexeS' tip and the debris, meeting the minimum required contact time, in constrast to non-adaptive strategy. The results validate the superiority of the adaptive scheme in achieving sufficient contact time and, consequently, the successful soft capture of uncooperative debris using gecko-adhesive pads in the presence of uncertainties.

VI. FUTURE STUDIES

Future studies will include the experimental validation and verification of the proposed controller using FlexeS in Zero-G Lab of SnT, University of Luxembourg [36]. The proposed controller will be integrated to ROS (Robot Operating System) infrastructure of Zero-G Lab.

ACKNOWLEDGMENT

A general overview of Zero-G Laboratory is available in the following video, named The Zero-G Laboratory: Testing in Micro-Gravity Environment. The Zero-G

Laboratory has been designed and built to emulate scenarios such as rendezvous, docking, capture, and other various interaction scenarios between separate spacecrafts. It is equipped with high-tech infrastructure, consisting of nearly space-representative lightning conditions, motion capture system, floating platforms [37], epoxy floor, rails with robots, and capability to integrate onboard computers and mount large mock-ups. These abilities allow researchers from both industry and academy to conduct a wide variety of experiments for unique orbital scenarios.

REFERENCES

[1] P. Bernhard, M. Deschamps, and G. Zaccour, "Large satellite constellations and space debris: Exploratory analysis of strategic management of the space commons," *Eur. J. Oper. Res.*, vol. 304, no. 3, pp. 1140–1157, Feb. 2023, doi: 10.1016/j.ejor.2022.04.030.

[2] C. Bonnal, J.-M. Ruault, and M.-C. Desjean, "Active debris removal: Recent progress and current trends," *Acta Astronautica*, vol. 85, pp. 51–60, Apr. 2013, doi: 10.1016/j.actaastro.2012.11.009.

[3] G. Borelli, G. Gaias, and C. Colombo, "Rendezvous and proximity operations design of an active debris removal service to a large constellation fleet," *Acta Astronautica*, vol. 205, pp. 33–46, Apr. 2023, doi: 10.1016/j.actaastro.2023.01.021.

[4] J. Drmola and T. Hubik, "Kessler syndrome: System dynamics model," *Space Policy*, vols. 44–45, pp. 29–39, Aug. 2018, doi: 10.1016/j.spacepol.2018.03.003.

[5] D. J. Kessler and B. G. Cour-Palais, "Collision frequency of artificial satellites: The creation of a debris belt," *J. Geophys. Res., Space Phys.*, vol. 83, no. A6, pp. 2637–2646, Jun. 1978, doi: 10.1029/ja083ia06p02637.

[6] H. Tomizaki, R. Kobayashi, M. Suzuki, N. Karasawa, S. Hasegawa, and K. Makihara, "Assessment of space debris collisions against spacecraft with deorbit devices," *Adv. Space Res.*, vol. 67, no. 5, pp. 1526–1534, Mar. 2021, doi: 10.1016/j.asr.2020.12.018.

[7] H. Hakima, M. C. F. Bazzocchi, and M. R. Emami, "A deorbiter CubeSat for active orbital debris removal," *Adv. Space Res.*, vol. 61, no. 9, pp. 2377–2392, May 2018, doi: 10.1016/j.asr.2018.02.021.

[8] NASA Safety Standard—Office of Safety and Mission Assurance. (1995). *Guidelines and Assessment Procedures for Limiting Orbital Debris, NASA NSS 1740*. [Online]. Available: https://ntrs.nasa.gov/citations/19960020946

[9] V. P. Blagun, S. V. Kulik, and V. I. Lukyashchenko, "Russian space agency activities on the problem of technogenic space debris," *Adv. Space Res.*, vol. 23, no. 1, pp. 271–274, Jan. 1999, doi: 10.1016/s0273-1177(99)00013-7.

[10] T. Takano, T. Tajima, T. Satoh, and Y. Arimoto, "Space debris measurements in Japan," *Adv. Space Res.*, vol. 23, no. 1, pp. 55–65, Jan. 1999, doi: 10.1016/s0273-1177(98)00230-0.

[11] H. Klinkrad, H. Sdunnus, and J. Bendisch, "Development status of the ESA space debris reference model," *Adv. Space Res.*, vol. 16, no. 11, pp. 93–102, Jan. 1995, doi: 10.1016/0273-1177(95)98757-f.

[12] T. D. Bess, "Mass distribution of orbiting man-made space debris," NASA, Washington, DC, USA, Tech. Rep. D-8108,1975, 8108. [Online]. Available: https://ntrs.nasa.gov/citations/19760007896

[13] M. Vasile, "Preface: Advances in asteroid and space debris science and technology—Part 1," *Adv. Space Res.*, vol. 56, no. 3, pp. 365–366, Aug. 2015, doi: 10.1016/j.asr.2015.05.031.

[14] H. Yoshida and M. Araki, "Social impact of space debris: Study of economic and political aspects," *Acta Astronautica*, vol. 34, pp. 345–355, Jun. 1994, doi: 10.1016/0094-5765(94)90271-2.

[15] D. Rex, "Will space run out of space? The orbital debris problem and its mitigation," *Space Policy*, vol. 14, no. 2, pp. 95–105, May 1998, doi: 10.1016/s0265-9646(98)00004-6.

[16] V. Aslanov and A. Ledkov, "Space debris problem," in *Attitude Dynamics and Control of Space Debris During Ion Beam Transportation*. Amsterdam, The Netherlands: Elsevier, 2023, pp. 53–112, doi: 10.1016/B978-0-323-99299-2.00004-5.

[17] B. C. Yalçın, C. Martinez, M. H. Delisle, G. Rodriguez, J. Zheng, and M. Olivares-Mendez, "ET-class: An energy transfer-based classification of space debris removal methods and missions," *Frontiers Space Technol.*, vol. 3, p. 23, Mar. 2022, doi: 10.3389/frspt.2022.792944.

[18] L. Yan, W. Xu, Z. Hu, and B. Liang, "Multi-objective configuration optimization for coordinated capture of dual-arm space robot," *Acta Astronautica*, vol. 167, pp. 189–200, Feb. 2020, doi: 10.1016/j.actaastro.2019.11.002.

[19] G. Fang, Y. Zhang, Y. Sun, and P. Huang, "On the stiffness selection for tethered space robot," in *Proc. IEEE Int. Conf. Robot. Biomimetics (ROBIO)*, Dec. 2022, pp. 297–302, doi: 10.1109/ROBIO55434.2022.10011953.

[20] N. R. Sinatra, C. B. Teeple, D. M. Vogt, K. K. Parker, D. F. Gruber, and R. J. Wood, "Ultragentle manipulation of delicate structures using a soft robotic gripper," *Sci. Robot.*, vol. 4, no. 33, Aug. 2019, doi: 10.1126/scirobotics.aax5425.

[21] X. Li, Z. Chen, and Y. Wang, "Detumbling a space target using soft robotic manipulators," in *Proc. IEEE Int. Conf. Mechatronics Autom. (ICMA)*, Aug. 2022, pp. 1807–1812, doi: 10.1109/ICMA54519.2022.9855912.

[22] M. Poozhiyil, M. H. Nair, M. C. Rai, A. Hall, C. Meringolo, M. Shilton, S. Kay, D. Forte, M. Sweeting, N. Antoniou, and V. Irwin, "Active debris removal: A review and case study on LEOPARD phase 0-A mission," *Adv. Space Res.*, vol. 72, no. 8, pp. 3386–3413, Oct. 2023, doi: 10.1016/j.asr.2023.06.015.

[23] S. Kayastha, J. Katupitiya, G. Pearce, and A. Rao, "Comparative study of post-impact motion control of a flexible arm space robot," *Eur. J. Control*, vol. 69, Jan. 2023, Art. no. 100738, doi: 10.1016/j.ejcon.2022.100738.

[24] Y. Zhang, J. Quan, P. Li, W. Song, G. Zhang, L. Li, and D. Zhou, "A flytrap-inspired bistable origami-based gripper for rapid active debris removal," *Adv. Intell. Syst.*, vol. 5, 2023, Art. no. 2200468, doi: 10.1002/aisy.202200468.

[25] S. Wu, F. Mou, Q. Liu, and J. Cheng, "Contact dynamics and control of a space robot capturing a tumbling object," *Acta Astronautica*, vol. 151, pp. 532–542, Oct. 2018, doi: 10.1016/j.actaastro.2018.06.052.

[26] M. H. Delisle, O.-O. Christidi-Loumpasefski, B. C. Yalçın, X. Li, M. Olivares-Mendez, and C. Martinez, "Hybrid-compliant system for soft capture of uncooperative space debris," *Appl. Sci.*, vol. 13, no. 13, p. 7968, Jul. 2023, doi: 10.3390/app13137968.

[27] N. Hogan, "Impedance control: An approach to manipulation," in *Proc. Amer. Control Conf.*, Jul. 1984, pp. 304–313, doi: 10.23919/ACC.1984.4788393.

[28] K. Koga and Y. Fukui, "Deorbiting of satellites by a free-flying space robot by combining positioning control and impedance control," in *Proc. 22nd Int. Conf. Control, Autom. Syst. (ICCAS)*, Nov. 2022, pp. 965–971, doi: 10.23919/ICCAS55662.2022.10003688.

[29] B. Dou, X. Yue, and T. Zhang, "Optimal detumbling strategy for a non-cooperative target with unknown inertial parameters using a space manipulator," *Adv. Space Res.*, vol. 69, no. 11, pp. 3952–3965, Jun. 2022, doi: 10.1016/j.asr.2022.03.017.

[30] F. Zhang, I. Sharf, A. Misra, and P. Huang, "On-line estimation of inertia parameters of space debris for its tether-assisted removal," *Acta Astronautica*, vol. 107, pp. 150–162, Feb. 2015, doi: 10.1016/j.actaastro.2014.11.016.

[31] T. C. Nguyen-Huynh and I. Sharf, "Adaptive reactionless motion and parameter identification in postcapture of space debris," *J. Guid., Control, Dyn.*, vol. 36, no. 2, pp. 404–414, Mar. 2013, doi: 10.2514/1.57856.

[32] J. J. E. Slotine and W. Li, *Applied Nonlinear Control*, vol. 199. Upper Saddle River, NJ, USA: Prentice-Hall, 1991.

[33] J. Brannan, N. Scott, and C. Carignan, "Robot servicer interaction with a satellite during capture," in *Proc. Int. Symp. Artif. Intell., Robot. Autom. Space*, Madrid, Spain, 2018.

[34] Z. Mitros, G. Rekleitis, I. Patsiaouras, and E. Papadopoulos, "Impedance control design for on-orbit docking using an analytical and experimental approach," in *Proc. 25th Medit. Conf. Control Autom. (MED)*, Valletta, Malta, Jul. 2017, pp. 1244–1249, doi: 10.1109/MED.2017.7984288.

[35] P. C. Hughes, *Spacecraft Attitude Dynamics*. Hoboken, NJ, USA: Wiley, 1986.

[36] M. Olivares-Mendez, M. R. Makhdoomi, B. C. Yalçın, Z. Bokal, V. Muralidharan, M. O. D. Castillo, V. Gaudilliere, L. Pauly, O. Borgue, M. Alandihallaj, J. Thoemel, E. Skrzypczyk, A. Rathinam, K. R. Barad, A. E. R. Shabayek, A. M. Hein, D. Aouada, and C. Martinez, "Zero-G lab: A multi-purpose facility for emulating space operations," *J. Space Saf. Eng.*, vol. 10, no. 4, pp. 509–521, Dec. 2023, doi: 10.1016/j.jsse.2023.09.003.

[37] B. C. Yalçın, C. Martinez, S. Coloma, E. Skrzypczyk, and M. A. Olivares-Mendez, "Lightweight floating platform for ground-based emulation of on-orbit scenarios," *IEEE Access*, vol. 11, pp. 94575–94588, 2023, doi: 10.1109/ACCESS.2023.3311202.

OLGA-ORSALIA CHRISTIDI-LOUMPASEFSKI received the Ph.D. degree from the National Technical University of Athens (NTUA), Greece. She worked on an ESA project as a Researcher and the Technical Project Manager of the CSL's Space Robotics Team, NTUA. Her doctoral research focused on dynamics and system identification of space robotic systems. She is currently a Research Associate with the SpaceR Research Group. Her current research interest includes active space debris removal.

BARIŞ CAN YALÇIN received the Ph.D. degree from the Mechatronics Engineering Department, Yildiz Technical University, Turkey, in 2019. He gained also working experience as a Research and Teaching Assistant with Yildiz Technical University. During the Ph.D. degree, he studied on the control theory topics and worked to design a novel control method to suppress micron-scale vibrations using magnetic levitation technology. Currently, he is with the Space Robotics Research Group (SpaceR), SnT—University of Luxembourg, headed by Prof. Miguel Angel Olivares Mendez, as a Research Associate/Postdoctoral Researcher. He is also researching space mechatronics domain to create various space related mechatronic systems, such as floating platforms and active/passive space debris removal systems. He is also a Designer of SpaceR-SnT's floating platform. He uses the floating platform for several research domains, such as close proximity, rendezvous, asteroid/planetary landing, and locomotion scenarios. In SpaceR, he contributes to ESA and FNR funded projects in which the floating platform plays a crucial role in realizing orbital robotic scenarios.

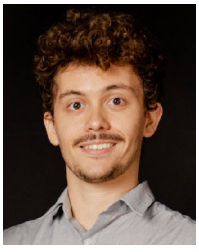

MAXIME HUBERT DELISLE is currently pursuing the Ph.D. degree with the Space Robotics Research Group, SnT—University of Luxembourg, designing a novel autonomous capturing solution for active debris removal of small uncooperative space debris. He is also a Mechatronic Engineer with Université de Technologie de Compigne, France, specialized in designing, controlling, and characterizing complex mechatronic systems, combining elements of mechanical engineering (design to prototype), electronics (sensors and actuators, robotics), and computer science (automation, ML, and data analysis). He is also working with ASML in The Netherlands on a DUV lithography project he gained experience in precision mechanics, prototyping, sensor acquisition and processing, thermal calculations, requirements definition, and thermal control modeling. His previous experience, expertise, and determination has led him to design a versatile hybrid-compliant mechanism to target a vast range of small uncooperative space debris in low earth orbit (LEO), enabling a profitable one-to-many solution.

XIAO LI is currently a Ph.D. Researcher with the Laboratory Space Robotics in Luxembourg City (SnT), University of Luxembourg. She is also working on HELEN project. Her research interests include mechatronics and computer science, focusing on mathematical modeling, multibody analysis and developing high-fidelity real-time in-orbit simulations (digital twins), and software-in-the-loop testing system for space missions.

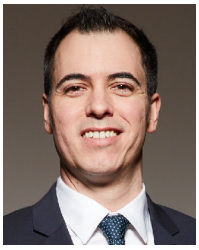

MIGUEL A. OLIVARES-MENDEZ (Member, IEEE) received the Eng. degree in computer science from the University of Malaga, in 2006, and the M.Sc. and Ph.D. degrees in robotics and automation from the Technical University of Madrid, in 2009 and 2013, respectively.

He is currently a tenured Assistant Professor in space robotics and a Senior Research Scientist with the Interdisciplinary Centre for Security, Reliability and Trust, University of Luxembourg (Uni.Lu). He leads the Space Robotics Research Group (SpaceR), the LunaLab, and the Zero-gravity Laboratory. During the Ph.D. degree, he was a Visitor Researcher with EPFL, Switzerland, and ARCAA-QUT, Australia. He was awarded with the 2013 Best Ph.D. Thesis Award by the European Society for Fuzzy Logic and Technology (EUSFLAT). In May 2013, he joined the Interdisciplinary Center for Security Reliability and Trust (SnT), Automation & Robotics Research Group, Uni.Lu, as an Associate Researcher. In December 2016, he became a Research Scientist and main responsible of the research activities on mobiles robotics with the Automation & Robotics Research Group, SnT—Uni.Lu. He is also a main supervisor of 11 Ph.D. students and seven postdoctoral students. He has published over 120 peer-reviewed publications. His main research interests include aerial, planetary and orbital robotics for autonomous navigation, situational awareness, perception, machine learning, multi-robot interaction in autonomous exploration, inspection, and operations.

Dr. Olivares-Mendez is an Associate Editor of IROS, ICRA, and ICUAS Conferences; and the *Journal of Intelligent & Robotics Systems*, *Frontiers on Space and Field Robotics*, and the *International Journal of Robotics Research*.

CAROL MARTINEZ is a Mechatronics Engineer from the UNAB (Colombia) and holds an MSc (2009) and a PhD (2013) in Robotics and Automation from the Universidad Politécnica de Madrid (UPM) in the area of Computer Vision for Unmanned Aerial Vehicles (visual tracking, pose estimation, and control), for which she received the outstanding PhD thesis award by the UPM. As a PhD candidate, she was a research visitor at the Queensland University of Technology and the University of Bristol, UK, where she developed algorithms for tracking and pose estimation using cameras on-board aerial vehicles. She has held positions as a Post-doctoral researcher at UPM and Assistant Professor at PUJ Bogotá, Colombia (2015-2020). She has led and conducted interdisciplinary research in Computer Vision, Machine Learning, and Deep Learning for process automation (industry and health) and robotics (aerial, industrial, and space).

Since 2020, she has been a Research Scientist at the SnT – University of Luxembourg (UniLu) in the Space Robotics Research Group, where she leads projects in orbital robotics (space debris removal, vision-based navigation), robotic manipulation (control, perception, and learning), and on-ground testing environment (the ZeroGLab facility). She is also a Lecturer in the Interdisciplinary Space Master (ISM) program at UniLu and provides guidance and supervision to PhD and Master researchers. Her research focuses on perception approaches for the autonomous operation of robots in space and multi-purpose manipulation tasks for planetary and orbital robotics applications.